NASA/CR—2015-218845

Near-Field Acoustic Power Level Analysis of F31/A31 Open Rotor Model at Simulated Cruise Conditions

Technical Report II

Dave Sree
Tuskegee University, Tuskegee, Alabama

July 2015

NASA STI Program . . . in Profile

Since its founding, NASA has been dedicated to the advancement of aeronautics and space science. The NASA Scientific and Technical Information (STI) Program plays a key part in helping NASA maintain this important role.

The NASA STI Program operates under the auspices of the Agency Chief Information Officer. It collects, organizes, provides for archiving, and disseminates NASA's STI. The NASA STI Program provides access to the NASA Technical Report Server—Registered (NTRS Reg) and NASA Technical Report Server—Public (NTRS) thus providing one of the largest collections of aeronautical and space science STI in the world. Results are published in both non-NASA channels and by NASA in the NASA STI Report Series, which includes the following report types:

- TECHNICAL PUBLICATION. Reports of completed research or a major significant phase of research that present the results of NASA programs and include extensive data or theoretical analysis. Includes compilations of significant scientific and technical data and information deemed to be of continuing reference value. NASA counter-part of peer-reviewed formal professional papers, but has less stringent limitations on manuscript length and extent of graphic presentations.

- TECHNICAL MEMORANDUM. Scientific and technical findings that are preliminary or of specialized interest, e.g., "quick-release" reports, working papers, and bibliographies that contain minimal annotation. Does not contain extensive analysis.

- CONTRACTOR REPORT. Scientific and technical findings by NASA-sponsored contractors and grantees.

- CONFERENCE PUBLICATION. Collected papers from scientific and technical conferences, symposia, seminars, or other meetings sponsored or co-sponsored by NASA.

- SPECIAL PUBLICATION. Scientific, technical, or historical information from NASA programs, projects, and missions, often concerned with subjects having substantial public interest.

- TECHNICAL TRANSLATION. English-language translations of foreign scientific and technical material pertinent to NASA's mission.

For more information about the NASA STI program, see the following:

- Access the NASA STI program home page at http://www.sti.nasa.gov

- E-mail your question to help@sti.nasa.gov

- Fax your question to the NASA STI Information Desk at 757-864-6500

- Telephone the NASA STI Information Desk at 757-864-9658

- Write to:
  NASA STI Program
  Mail Stop 148
  NASA Langley Research Center
  Hampton, VA 23681-2199

NASA/CR—2015-218845

Near-Field Acoustic Power Level Analysis of F31/A31 Open Rotor Model at Simulated Cruise Conditions

Technical Report II

Dave Sree
Tuskegee University, Tuskegee, Alabama

Prepared under Contract NNC13BA10B

National Aeronautics and
Space Administration

Glenn Research Center
Cleveland, Ohio 44135

July 2015

Acknowledgments

The present work was sponsored by the NASA Environmentally Responsible Aviation Project Propulsion subtask, with Ken Suder as Project Monitor. This work was performed under the Universities Space Research Association (USRA)'s Advanced Research and Technology Support Task Order, IDIQ Subcontract Number 04555-014 (Prime Contract Number NNC13BA10B) for NASA Glenn Research Center. The support from USRA and Acoustics Branch at NASA GRC is greatly appreciated. The author would like to thank Dr. David B. Stephens of the Acoustics Branch for all his help, suggestions, and fruitful discussions.

Level of Review: This material has been technically reviewed by NASA technical management.

Available from

NASA STI Program
Mail Stop 148
NASA Langley Research Center
Hampton, VA 23681-2199

National Technical Information Service
5285 Port Royal Road
Springfield, VA 22161
703-605-6000

This report is available in electronic form at http://www.sti.nasa.gov/ and http://ntrs.nasa.gov/

Preface

The second part of the task under this Universities Space Research Association (USRA) subcontract number 04555-014 involved performing and documenting the near-field acoustic power level analysis of open rotor model F31/A31 at simulated cruise conditions based on data obtained from high-speed wind tunnel (SWT) tests at NASA Glenn Research Center (NASA GRC). The nonproprietary portions of the test data were provided by NASA GRC to perform the task. This subcontractor's report on the second part of the task is provided in the form of *Technical Report II* which consists of relevant sound power level results from the analysis and their detailed discussions. The technical report is included as an attachment to this summary. The deliverables, namely, revised technical report, data analysis codes, spreadsheets of results, tables, figures, etc. will be shipped to the technical monitor at NASA GRC in electronic form at the end of the contract period.

Near-Field Acoustic Power Level Analysis of F31/A31 Open Rotor Model at Simulated Cruise Conditions

Technical Report II

Dave Sree
Tuskegee University
Tuskegee, Alabama 36088

Summary

Near-field acoustic power level analysis of F31/A31 open rotor model has been performed to determine its noise characteristics at simulated cruise flight conditions. The nonproprietary parts of the test data obtained from experiments in the 8- by 6-Foot Supersonic Wind Tunnel (8×6 SWT) were provided by NASA Glenn Research Center. The tone and broadband components of total noise have been separated from raw test data by using a new data analysis tool. Results in terms of sound pressure levels, acoustic power levels, and their variations with rotor speed, freestream Mach number, and input shaft power, with different blade-pitch setting angles at simulated cruise flight conditions, are presented and discussed. Empirical equations relating model's acoustic power level and input shaft power have been developed. The near-field acoustic efficiency of the model at simulated cruise conditions is also determined. It is hoped that the results presented in this work will serve as a database for comparison and improvement of other open rotor blade designs and also for validating open rotor noise prediction codes.

Nomenclature

AOA	Angle of attack
BSA	Blade-pitch setting angles
H	Sensor proximity height
M, M_0	Freestream Mach number
OAPWL	Overall power watt level
OASPL	Overall sound pressure level
P_{ac}	Measured acoustic power
P_{ref}	Reference acoustic power
P_{spb}	Input shaft power per blade
PWL	Power watt level
R^2	Goodness-of-fit parameter
R_{aft}	Aft rotor radius
SPL	Sound pressure level

1.0 Introduction

In this case, the term "open rotor" refers to an unducted counter-rotating twin rotor model which is being considered as a propulsion device for future aircraft (Refs. 1 and 2). Open rotors are also known as "propfans." Open-rotor propulsion technology is now being developed as a viable alternative to modern day turbofan engines mainly because of predicted fuel economy benefits and improved performance (Ref. 3). However, high noise levels associated with open rotors pose both environmental and technological challenges. These include community noise around airports, passenger discomfort, aircraft structural integrity, and meeting stringent federal noise regulations.

NASA Glenn Research Center (NASA GRC), in collaboration with the U.S. aircraft industry, has been conducting both analytical and experimental research studies to address this noise issue and to develop improved open rotor systems (Ref. 4). Tests on scale-model systems have been conducted in low- and high-speed wind tunnels at NASA GRC to understand the noise mechanisms and evaluate the acoustic performance of open rotors. Large amounts of both far-field and near-field acoustic data have been collected during an extensive test campaign from 2009 to 2012 to determine the noise levels under various simulated flight conditions (Refs. 5 to 7). The open rotor model used for testing was a one-fifth scale model having a so-called "historical" baseline blade set made of carbon fiber composite with a metal spar. This blade set is designated as "F31/A31" and serves as a nonproprietary baseline design for comparison with other blade designs (Refs. 5 to 7).

Near-field acoustic tests on the model were carried out in the 8- by 6-Foot (high-speed) or Supersonic Wind Tunnel (SWT) at NASA GRC to study the model noise characteristics at simulated cruise flight conditions. Tests were conducted at various rotor speeds and freestream Mach numbers (M) with different blade-pitch setting angles (BSA) to conduct a parametric study of the model noise levels.

Initial investigations of the test data of F31/A31 model have been reported by Stephens (Refs. 6 and 7) in terms of narrowband noise spectra, sound pressure levels (SPL), and overall sound pressure levels (OASPL) for simulated cruise condition at M = 0.78 with BSA = 64.4°/61.8° forward/aft rotor case. These investigations were based on the overall noise levels only. No attempts were made to separate the tone and broadband noise components from raw test data. No proper data processing tools were available at the time to separate tone and broadband noise. It is reported by Stephens (Refs. 6 and 7) that the measured unsteady pressure data at simulated cruise conditions in the 8- by 6-Foot Supersonic Wind Tunnel were mostly tone-dominated. Based on comparisons of overall noise spectra with extensive database on tare (or background) noise spectra, he found that the broadband components were interfered by the background noise for frequencies below about 3,200 Hz. It is also believed that the broadband components in the measured data were swamped by the tunnel flow over the sensors, particularly at close proximities to the rotors. Thus, determination of the tone component of the noise became very important.

It is known that the open rotor total or overall noise consists of both tonal and broadband components. (The terms 'total' and 'overall,' and 'tonal' and 'tone,' will be used interchangeably in this report.) The determination of tonal and broadband noise components from raw acoustic test data is very important for properly assessing the noise control parameters and also for validating the open rotor noise prediction codes (Refs. 8 to 10). A new data processing method developed by Sree (Ref. 11) is now available to separate the tonal and broadband noise components from raw experimental data of open rotors. This method will be applied to examine the tone and broadband noise levels of the F31/A31 model. Because the model noise, as mentioned above, is mostly tone-dominated, much focus will be placed on presenting the tone noise characteristics in this report.

The main purpose of the present work is to analyze the near-field experimental data available on F31/A31 and report the tone noise results together with total noise in a few selected cases. Some portions of the test data are declared nonproprietary and are provided by NASA GRC to perform the task. The noise levels will be expressed in terms of SPL and power watt level (PWL) at simulated cruise conditions. Variations of the noise levels with rotor speed, freestream Mach number, measurement location, blade-pitch setting angles, and input shaft power will be studied. Correlation of PWL with input shaft power will be developed to study the acoustic performance of the model. It is hoped that the results presented here will serve as a valuable database for comparing other open rotor blade designs with F31/A31 and also for validating open rotor noise simulation codes.

2.0 F31/A31 Model and the Test Rig

A detailed description of the F31/A31 model and the test rig is given by Elliott (Ref. 5) and Stephens (Refs. 6 and 7). However, a few salient features of the model will be worth repeating here. The F31/A31 model has two counter-rotating rotors. The axial distance between their pitch axes is 19.9 cm (7.8 in.). The forward rotor is approximately 65.2 cm (25.7 in.) in diameter and has 12 blades whereas the aft rotor

Figure 1.—Photograph of F31/A31 model and ORPR test rig installed in the 8×6 SWT; (Courtesy: Acoustics Branch, NASA GRC).

is approximately 63.0 cm (24.8 in.) in diameter and has 10 blades. The hub diameter of the forward rotor is approximately 26.6 cm (10.5 in.) and that of the aft rotor is 24.6 cm (9.7 in.). The pitch of the rotor blades could be adjusted to provide different operating conditions at cruise.

For all the tests conducted in the 8- by 6-Foot Supersonic Wind Tunnel, the F31/A31 model was mounted on a test rig called the "Open Rotor Propulsion Rig (ORPR)" in a simulated pusher-type arrangement (Refs. 6 and 7). The model was tested in an isolated configuration, without an upstream pylon. The turbines within the test rig were fed by high pressure air at about 20 atm (300 psi) to turn the rotor blades. All test runs were made at zero angle of attack (AOA) relative to the longitudinal axis of the model. A photograph of the model and the test rig installed for test in the 8- by 6-Foot Supersonic Wind Tunnel is shown in Figure 1.

3.0 Near-Field Sideline Acoustic Measurements

The near-field sideline acoustic measurements in the 8- by 6-Foot Supersonic Wind Tunnel were performed at various simulated cruise conditions. The tests were conducted using three different BSA with varying freestream Mach numbers and rotor speeds. These details will be given in the next section. An aluminum plate with 17 flush-mounted unsteady pressure measuring transducers (Refs. 6 and 7) was used to collect data simultaneously at seventeen axial locations parallel to and above the model's (centerline) longitudinal axis (Fig. 2). The plate can be seen in Figure 1. The plate could be remotely lowered from the wind tunnel ceiling to achieve various near-field sideline distances or sensor proximity heights (H) from the model's axis of rotation. The height could be varied from 42.65 to 116.08 cm. The geometric and acoustic emission directivity angles corresponding to the seventeen axial locations depend on H and M (Refs. 6 to 7). For example, their values, relative to aft rotor pitch change axis, for H = 50.85 cm and 116.08, and M = 0.78 are given in Table 1. Note that the angles are measured from upstream with respect to the longitudinal axis of the model. The near-field unsteady pressure data at these locations were collected using a sampling frequency of 200 kHz. The data record length for each test run was 15 sec.

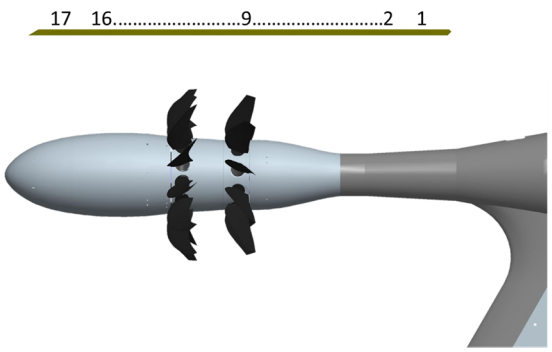

Figure 2.—Illustration showing the seventeen measurement locations above the model and relative to aft rotor pitch change axis; (Courtesy: Acoustics Branch, NASA GRC).

TABLE 1.—SEVENTEEN SENSOR AXIAL LOCATIONS AND THEIR CORRESPONDING GEOMETRIC AND ACOUSTIC EMISSION ANGLES RELATIVE TO AFT ROTOR PITCH CHANGE AXIS AT H = 50.85 cm AND 116.08 cm, AND M = 0.78

		H=50.85 cm	H=50.85 cm	H=116.08 cm	H=116.08 cm
Sensor Number	Sensor Axial Location (cm)	Geometric Angle (degree)	Acoustic Emission Angle (degree)	Geometric Angle (degree)	Acoustic Emission Angle (degree)
1	-46.6	132.5	97.4	111.9	65.5
2	-39.0	127.5	89.3	108.6	60.9
3	-34.1	123.9	83.5	106.4	57.9
4	-29.6	120.2	77.8	104.3	55.2
5	-23.5	114.8	69.7	101.4	51.6
6	-18.9	110.4	63.4	99.2	48.9
7	-14.8	106.3	57.8	97.3	46.6
8	-7.0	97.8	47.3	93.5	42.3
9	0.0	90.0	38.7	90.0	38.7
10	7.0	82.2	31.6	86.5	35.4
11	14.8	73.7	25.3	82.7	32.0
12	18.9	69.6	22.6	80.8	30.4
13	23.5	65.2	20.1	78.6	28.7
14	29.6	59.8	17.4	75.7	26.6
15	34.1	56.1	15.8	73.6	25.2
16	39.0	52.5	14.3	71.4	23.7
17	46.6	47.5	12.4	68.1	21.7

TABLE 2.—TEST CONFIGURATIONS FOR F31/A31 MODEL IN THE 8×6 SWT

Simulated Flight Condition	Blade-pitch Setting Angles (BSA)	Freestream Mach Number (M)	% Rotor Design Speed Range	Measurement Height (H) from Model's Longitudinal Axis, cm
Cruise (AOA = 0°) (No Pylon)	60.5°/59.0°	0.67 0.73 0.78 0.80 0.85	81.6 to 110.2	42.65 50.85 69.11 87.38 116.08
	62.9°/60.5°	0.73 0.78 0.80 0.85	77.5 to 100.1	42.65 50.85 69.11 87.38 116.08
	64.4°/61.8°	0.73 0.78 0.80 0.85	70.0 to 100.0	42.65 50.85 69.11 87.38 116.08

4.0 Test Configurations

The test configurations for the model at simulated cruise flight conditions are summarized as shown in Table 2. Three cases of blade-pitch setting angles (forward/aft) were considered: (1) BSA = 60.5°/59.0°, (2) BSA = 62.9°/60.5°, and (3) BSA = 64.4°/61.8°. These cases were chosen in order to obtain the best aerodynamic performance of the system at a given shaft speed and freestream Mach number. The Mach number variations ranged from 0.73 to 0.85 except for case (1) where they ranged from 0.67 to 0.85. (Tests conducted at other Mach numbers are not considered in this report.) All tests were performed by operating both rotors at the same speed. The rotor speeds were varied differently from 70 percent to about 110 percent of corrected design speed depending upon BSA, as shown in Table 2. The corrected rotor design speed was taken as 7516 rpm. All tests were performed with AOA set to zero. Five sensor proximity heights (H) were chosen for data collection and are also given in Table 2. At each height, seventeen axial unsteady pressure measurements were made simultaneously. As mentioned earlier, data were collected for 15 sec, for each test run, using a sampling frequency of 200 kHz.

5.0 Results and Discussion

Special data processing techniques were applied to the near-field acoustic data obtained from simulated cruise tests in the high-speed wind tunnel. The new technique developed by Sree (Ref. 11) was used to separate the tone and broadband noise components from the raw data. Noise levels of each component were computed in terms of SPL and PWL, and as a function of rotor speed, Mach number, and measurement location for each BSA case. The main focus will be on presenting the tone noise characteristics here.

Since the test cases and the range of operating conditions were large, and the number of outcomes many, only selected results of SPL and PWL will be presented in this report. The results obtained at various rotor speeds with BSA = 64.4°/61.8° and M = 0.78 were of particular interest. A large number of interesting measurements were made at this operating condition. Also, these results are representative of similar results obtained in the other two BSA cases. However, some results of PWL variation with rotor speed at M = 0.78 will also be presented to compare the differences in PWL among the three BSA cases.

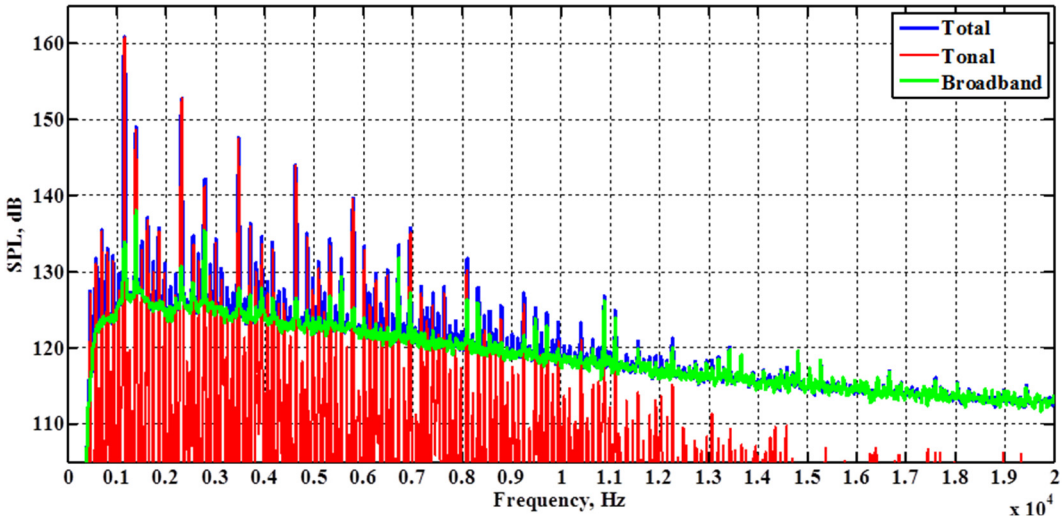

Figure 3.—Narrowband noise spectra of overall and the corresponding tonal and broadband components at simulated cruise condition (sensor #9); BSA = 64.4°/61.8°, 91.1 percent design rotor speed, M = 0.78, H/R_{aft} = 1.61.

5.1 Narrowband Noise Power Spectra

As stated earlier, the total, tonal, and broadband narrowband noise spectra were first determined using the method developed by Sree (Ref. 11). The spectral analysis was performed using a sample size of 3 million and a frequency resolution of 12.2 Hz. In order to avoid the interference of wind tunnel background noise, particularly at low rotor speeds, the raw data was pre-processed using a 500 Hz to 50 kHz band-pass filter before the spectral analysis was carried out. The background noise in the 8- by 6-Foot Supersonic Wind Tunnel has already been addressed by Stephens (Refs. 6 and 7), and Sree and Stephens (Ref. 12).

An example of the narrowband spectra of the overall (blue), tonal (red), and broadband (green) noise components is shown in Figure 3. These spectra were computed from the data measured by sensor #9 at H = 50.85 cm (or H/R_{aft} = 1.61 where R_{aft} is aft rotor radius) under simulated cruise condition at M = 0.78 and 91.1 percent rotor design speed. Sensor #9 is in line with the aft rotor pitch change axis, i.e., at 90° geometric (or 38.7° acoustic emission) angle from aft rotor center (see Table 1). The spectral values are given in terms of SPL, in dB (referenced to 20 μPa), as a function of frequency, in Hz. The results show the rotor alone and other interaction tones from the two rotors at respective blade passing frequencies. They also reveal that the data is very much tone-dominated, as has been previously evidenced by Stephens (Refs. 6 and 7) also.

It is also seen from this example that the tone noise is dominant in the 1 to 11 kHz range. The tone and broadband components are reasonably well separated except for a few spikes in the broadband spectrum. Notice that these spike levels are well below their corresponding (major) tonal levels. The spikes are attributed to random phase shifts and modulations in narrow tonal frequencies in the measured signal due to unsteadiness or jitter in rotor speeds, particularly at higher shaft speeds. Measured signals also get distorted by other extraneous effects. The new data processing technique by Sree is not able to eliminate the spikes completely. This is one of the limitations of the new technique, particularly at higher shaft speeds with jitter (Ref. 12).

5.2 Integrated Sound Pressure Levels Versus Rotor Speed

The sound pressure levels were computed by integrating the spectral results from 500 Hz to 50 kHz. Results from selected test data only will be presented here. As mentioned before, only the tone noise results will be presented here. (The broadband SPL generally varied between 150 and 155 dB).

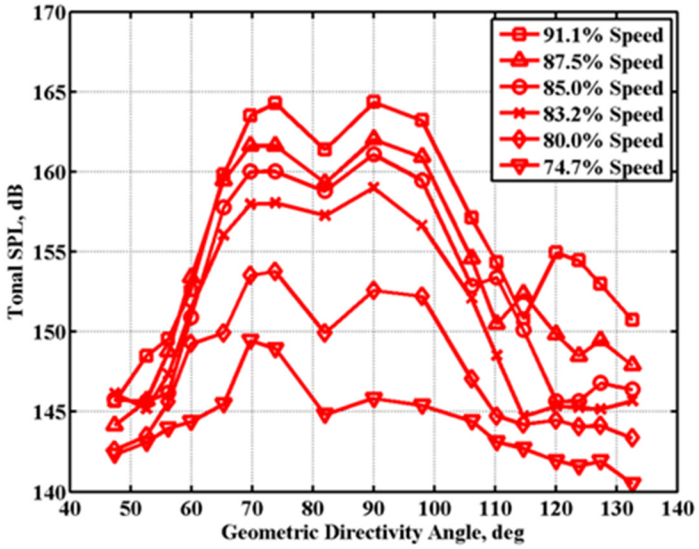

Figure 4.—Integrated SPL of tone noise as a function of geometric directivity angle for various rotor design speeds; BSA = 64.4°/61.8°, M = 0.78, H/R_{aft} = 1.61.

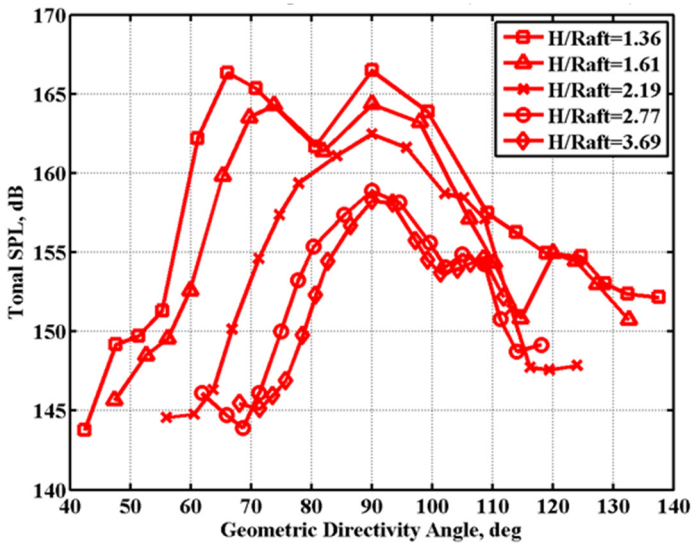

Figure 5.—Integrated SPL of tone noise as a function of geometric directivity angle for different sensor proximity heights; BSA = 64.4°/61.8°, M = 0.78, 91.1 percent rotor design speed.

The computed tonal SPL results from data obtained at M = 0.78 and H/R_{aft} = 1.61 for the BSA = 64.4°/61.8° case are shown in Figure 4. They are plotted as a function of geometric directivity angle, relative to aft rotor pitch change axis, for different rotor speeds ranging from 74.7 to 91.1 percent design speed. It is seen from these results that the SPL is directly proportional to the rotor speed. The tonal SPL rises sharply to about 165 dB around the rotors. Also noticed is a “dip” in the SPL for axial locations in between the rotors at this proximity height of H/R_{aft} = 1.61.

5.3 Integrated Sound Pressure Levels Versus Sensor Proximity Height

The integrated SPL was also computed for different sensor proximity heights at a given rotor speed. Figure 5 shows the tonal SPL variations with H/R_{aft} for the case where both rotors were running at 91.1 percent design speed. The x-axis shows the geometric sound directivity angles, in degrees. As one

would expect, the tonal SPL steadily increases as the sensor translating plate moves closer to the rotors. When moved very close to the rotors (i.e., at H/R_{aft} = 1.36 and 1.61), a "dip" in the SPL occurs for axial locations in between the rotors, the tonal SPL is in the range of 144 to 167 dB.

5.4 Acoustic Power Levels

Sound or acoustic power is sonic energy per unit time and is measured in Watts (W). The sound power level, sometimes, is expressed as Power Watt Level (PWL) in dB units. PWL is a logarithmic measure of the sound power level in comparison to a reference level of 10^{-12} W, i.e., $PWL_{dB} = 10 \log_{10} (P_{ac}/P_{ref})$ where P_{ac} = measured acoustic power in W and $P_{ref} = 10^{-12}$ W.

In this work, the acoustic power level, Π (or PWL), was calculated by assuming the measured sideline pressures were in the acoustic far-field. Spherical spreading was assumed to map the sideline measurement on to a constant radius arc. The following equation, which takes into account the tunnel or freestream Mach number effect, was used to compute the PWL (Ref. 13):

$$\Pi = \frac{2\pi d^2}{\rho_0 c_0} \int_0^{\pi} (1 - M_0 \cos\theta_e)^2 \frac{\overline{p'^2}(d, \theta_g)}{\sin\theta_e} d\theta_e$$

where

d	sideline distance from model centerline,
ρ_0	ambient air density,
c_0	speed of sound,
M_0	tunnel or freestream Mach number,
θ_e	sound emission angle,
θ_g	geometric (measurement) angle, and
$\overline{p'^2}(d,\theta_g)$	time-averaged sideline mean-squared pressure at measurement angle, θ_g,

[Note: $\theta_e = \theta_g - \sin^{-1}(M_0 \sin\theta_g)$]

The acoustic intensity at each rotor speed was calculated using the information from corresponding narrowband spectra and was integrated over frequencies between 500 Hz and 50 kHz. The intensity was assumed to be symmetric about the axis of the model and integrated over the portion of the spherical surface spanned by the sideline measurement angles. The upstream and downstream portion beyond the measurement angle was excluded from the calculation. The span of the directivity angles, however, is limited due to very close proximity of the measurement locations in the 8-by 6-Foot Supersonic Wind Tunnel and may not satisfy the far-field and spherical distribution assumptions in PWL calculations. The presence of the overhead sensor plate may also have some influence on the final results. The computed PWL may be questionable, but, unfortunately, there are no similar data available at present to compare and verify them.

5.4.1 PWL Versus Sensor Proximity Height; Effect of Rotor Speed

PWL of the model's noise components was computed as a function of sensor proximity height (H) for different rotor speeds at simulated cruise conditions. Here again, the emphasis will be placed on tone noise only. (The broadband PWL generally varied between 152 and 156 dB.) The tonal PWL results for the case of BSA = 64.4°/61.8° and M = 0.78 are given in Figure 6. Similar results were obtained for the other two BSA cases. Note on the x-axis in Figure 6, H is normalized with respect to aft rotor radius, R_{aft}. It is seen from these results that, for a given rotor speed, the PWL does not change very much with proximity heights. However, for a given H, the PWL increases significantly as the rotor speed is increased.

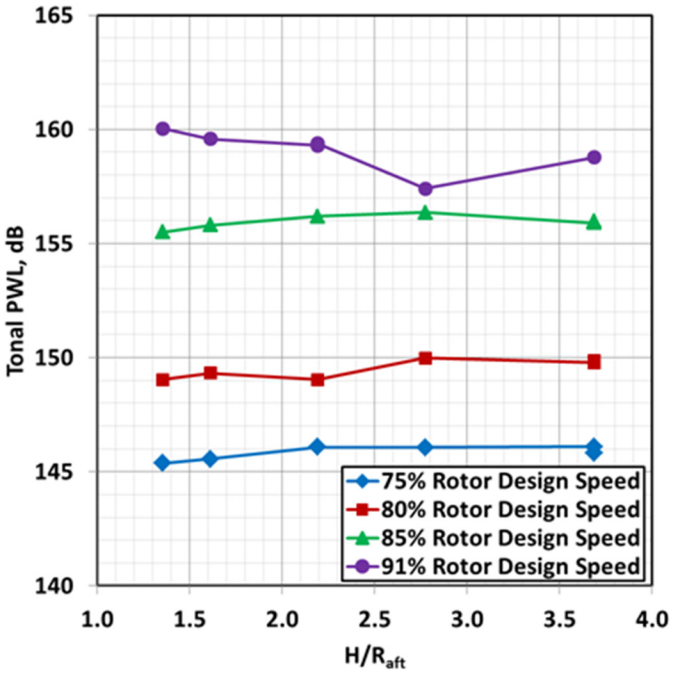

Figure 6.—PWL of tone noise as a function of sensor proximity height at different rotor design speeds; BSA = 64.4°/61.8°, M = 0.78.

5.4.2 PWL Versus Rotor Speed; Effect of Freestream Mach Number

We noticed from the results just presented in Figure 6 that the tonal PWL values do not significantly change with H for a given rotor speed. The change is less than about 2 dB. A large number of measurements were made at H = 116.08 cm (or H/R_{aft}= 3.69) compared to other H locations. Enough data were available at this H location so that meaningful results of PWL versus rotor speed can be presented at different Mach numbers. These results of tone noise are shown in Figure 7 for the BSA = 64.4°/61.8° case. The results reveal that the PWL steadily increases as the rotor speed is increased. For any given rotor speed, there is less than 3 dB change in PWL as M is increased. The PWL seems to level off to about 159 dB beyond about 90 percent design speed. It is also seen that, for speeds greater than 85 percent design speed, PWL at M = 0.85 (purple) is lower than those at other Mach numbers.

5.4.3 PWL Versus Rotor Speed; Effect of Blade-Pitch Setting Angles

So far all the results that have been presented are for the BSA = 64.4°/61.8° case only. However, it was also of interest to compare and study the differences in PWL among the three BSA cases considered in the simulated cruise test program (see Table 2). This comparison is done as shown in Figure 8 for a given M of 0.78. (The results are similar at other given Mach numbers also.) Figure 8 shows the tonal PWL as a function of rotor design speed for the three BSA cases. The data do not overlap and show some differences in each case. In general, the PWL increases with increasing speed in each case. The BSA = 64.4°/61.8° case seems to have higher noise levels than the other two. Note that the rotor speed ranges tested were different for each case. In the 85 to 90 percent speed range, the maximum difference of the tone noise between BSA = 64.4°/61.8° and BSA = 60.5°/59.0° cases is about 8 dB.

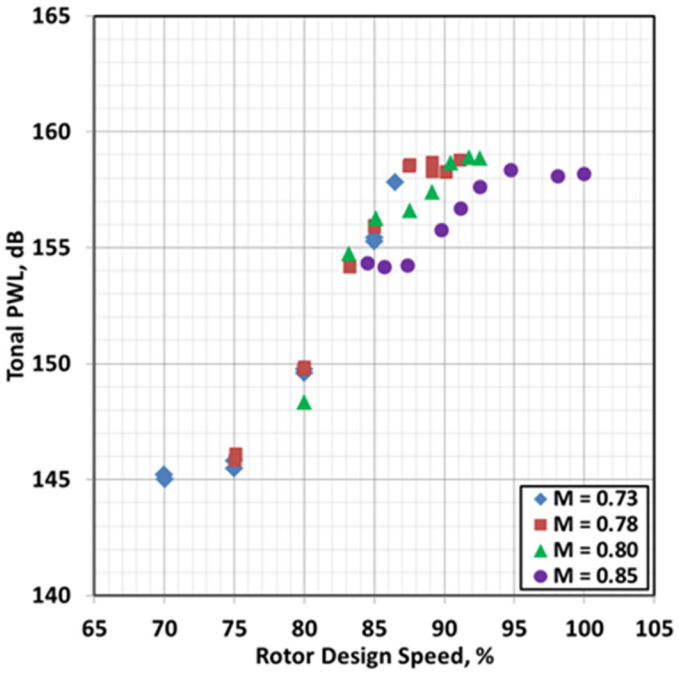

Figure 7.—PWL of tone noise as a function of rotor speed at different freestream Mach numbers; BSA = 64.4°/61.8°, H/R_{aft} = 3.69.

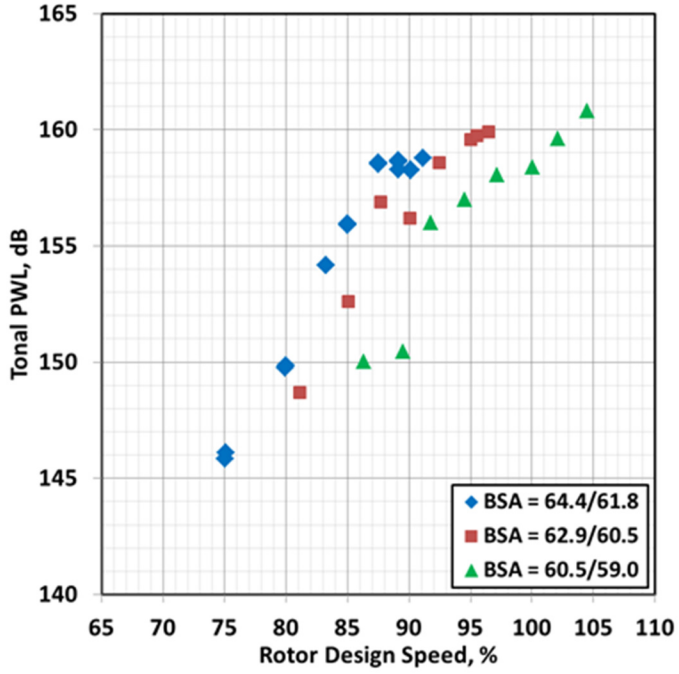

Figure 8.—PWL of tone noise as a function of rotor design speed at three different BSA; M = 0.78, H/R_{aft} = 3.69.

5.5 Overall PWL Versus Input Shaft Power

Relation between total emitted sound power level and input shaft power is always of interest when dealing with aeroacoustics of flying machines. This relation is shown in Figure 9 for the BSA = 64.4°/61.8° case at M = 0.78 and 0.80 only because good correlation was observed at these Mach numbers. (The data gets too scattered when all Mach number cases are included in the plot.) Also, the results shown in this figure are for the proximity height $H/R_{aft} = 3.69$. Similar results can be obtained for other BSA cases also. Janardan and Gliebe (Ref. 13) found a good correlation between overall PWL (OAPWL) and input shaft power for one of the earlier open rotor models they tested. They suggested to use a plot of overall PWL as a function of shaft power per blade, or $\log_{10}$ (shaft power per blade), to obtain a good indication of blade loading for a given input shaft power. Both types of plots are presented in Figure 9 for the F31/A31 model. As seen from these results, a good correlation between OAPWL and input shaft power is observed. Using regression analysis, polynomial curve-fits of the form:

$$OAPWL = - 0.00167\ P_{spb}^2 + 0.2653\ P_{spb} + 151.3955 \quad (1)$$

with $R^2 = 0.9613$ is found for the results in Figure 9(a), and

$$OAPWL = 7.4407\ P_{spb}^2 - 10.7878\ P_{spb} + 157.4165 \quad (2)$$

with $R^2 = 0.9589$ is found for the results in Figure 9(b). In both of these equations, P_{spb} stands for input shaft power per blade, in kW, and OAPWL is in dB. Based on the actual results obtained in this work, the maximum error associated with these empirical equations is found to be less than 1 dB. Similar correlations can be obtained for tonal and broadband PWL also.

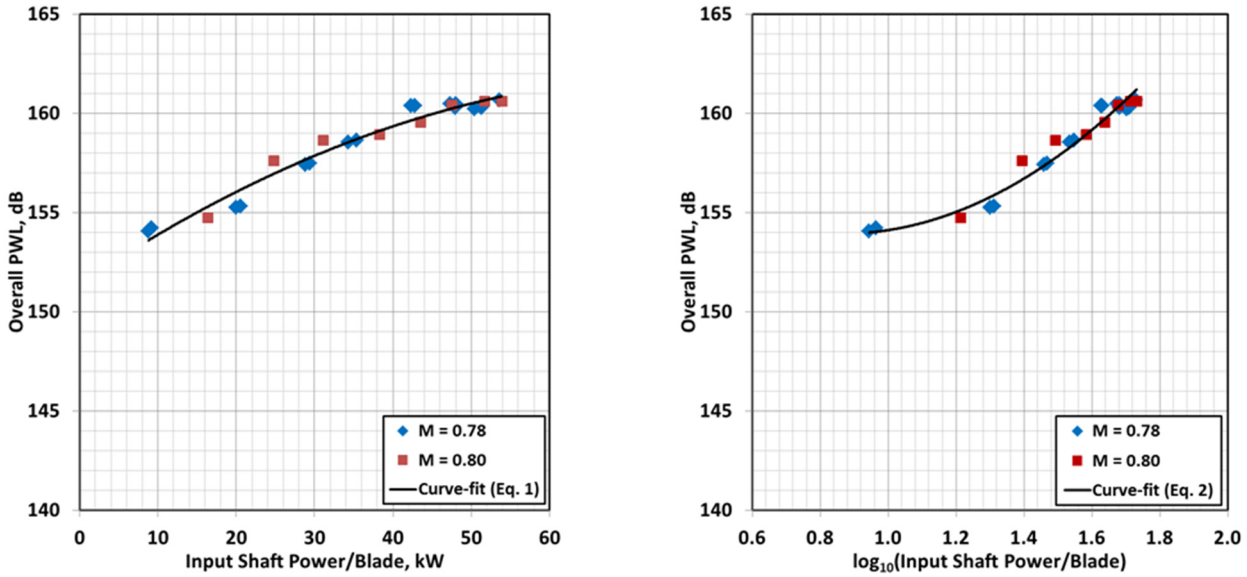

(a) OAPWL vs Shaft Power/Blade (b) OAPWL vs $\log_{10}$ (Shaft Power/Blade)

Figure 9.—Variation of overall PWL with input shaft power for BSA = 64.4°/61.8° case; M = 0.78 and 0.80, $H/R_{aft} = 3.69$.

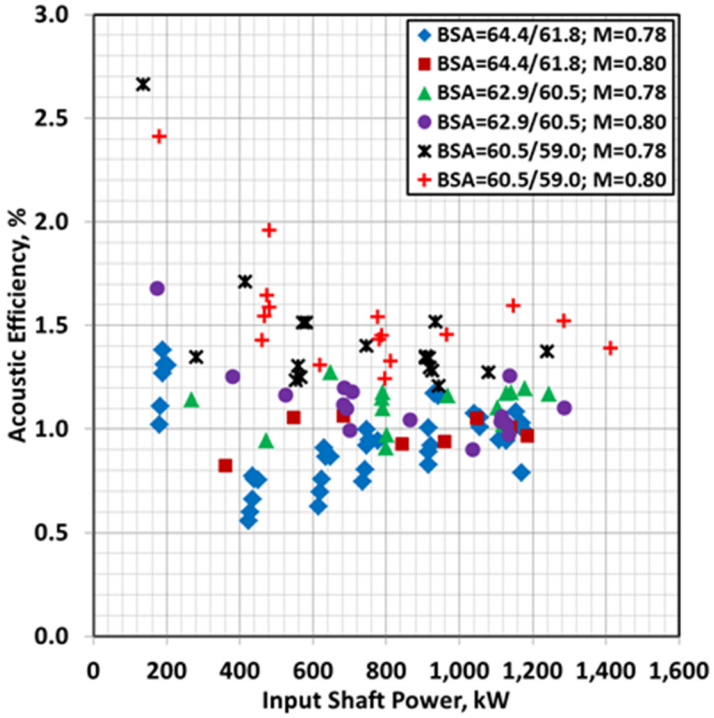

Figure 10.—Acoustic efficiency as a function of input shaft power for three BSA cases at simulated cruise condition; M = 0.78 and 0.80.

5.6 Acoustic Efficiency

The acoustic efficiency is defined as the ratio of the radiated acoustic power to the input shaft power where the radiated acoustic power is taken as the OAPWL (Refs. 14 and 15). Both powers are taken in kilowatt units in this work. Based on computed OAPWL values for the three BSA cases with M = 0.78 and 0.80 in the 8- by 6-Foot Supersonic Wind Tunnel, the near-field acoustic efficiency for the F31/A31 model is found to be below about 2.7 percent, as shown in Figure 10. However, for the BSA = 64.4°/61.8° case (blue symbols) this efficiency is less than 1.4 percent. The validity of these efficiencies has not been verified yet.

6.0 Conclusions

Analysis of near-field sound pressure levels and acoustic power levels of the open rotor model F31/A31 at simulated cruise flight conditions has been presented in this work. The analysis was performed on the nonproprietary portions of the test data provided by NASA-GRC. The model's acoustic tests at simulated cruise conditions were conducted in the 8- by 6-Foot Supersonic Wind Tunnel facility at NASA-GRC. Test configurations consisted of three blade-pitch settings with varying rotor speeds, freestream Mach numbers, and sideline measurement locations. Both rotors were running at the same speed and the angle of attack was set to zero in all the test configurations.

A new data analysis technique has been successfully applied to separate the tone and broadband noise components from the measured raw data to understand their level of contribution to the total noise. Since much of the measured unsteady pressure signals were dominated by tone noise, emphasis was placed on presenting mainly the tone noise characteristics. (The broadband SPL and PWL were found to be generally in the range of 150 to 156 dB, but they were believed to be marred by the tunnel flow over the sensors.) Computed SPL and PWL and their variations with rotor speed, freestream Mach number, measurement location, and input shaft power have been presented and discussed.

The results show that the near-field tonal SPL is directly proportional to rotor operating speed and measurement proximity. They dominate around the rotors. The tonal SPL is in the range of 140 to 167 dB. The tonal PWL is also directly proportional to the rotor speed. However, no significant changes in the tonal PWL are found as the measurement proximity is increased toward the rotors. The tonal PWL is in the range of 145 to 161 dB. At any given rotor speed, the freestream Mach number causes only small changes in PWL, except for the 85 to 90 percent design speed range where up to 5 dB differences are observed. For a given blade-pitch setting and proximity height, the noise results at M = 0.78 and 0.80 have similar characteristics. At any given Mach number and proximity height, the noise levels resulting from higher blade-pitch setting are found to be slightly higher than those from lower settings at all rotor speeds, except for the 85 to 90 percent design speed range where the differences are found to be as much as 8 dB.

Based on good correlation, empirical relations between the model's overall PWL and input shaft power have been developed. The SWT test results for the three BSA cases with M = 0.78 and 0.80 show that the near-field acoustic efficiency of the model is less than about 2.7 percent.

Lastly, it is hoped that the results presented in this work will serve as a good database for comparison and improvement of other open rotor blade designs as well as for validating open rotor noise prediction codes.

References

1. "Building a Better Plane," NASA News & Features, May 3, 2010, URL: http://www.nasa.gov/topics/aeronautics/features/openrotor_prt.htm [cited 3 May 2010].
2. James, T., "Back to Propellers," Engineering and Technology Magazine, Volume 4, Issue 10, 2 June 2009. URL: http://eandt.theiet.org/magazine/2009/10/back-to-propellers.cfm [cited 2 June 2009].
3. "Fuel prices drive new look at open rotor jet engines," Engineering and Technology Magazine, 27 October 2008. URL: http://eandt.theiet.org/news/2008/oct/open-rotor-test.cfm [cited 27 October 2008].
4. "GE and NASA Partner on Open Rotor Engine Testing," NASA-Ask the Academy, Volume 2, Issue 3, 30 March 2009. URL: http://www.nasa.gov/offices/oce/appel/ask-academy/issues/volume2/AA_2-3_F_ge_rotor.html [cited 30 March 2009].
5. Elliott, D.M., "Initial Investigation of the Acoustics of a Counter Rotating Open Rotor Model with Historical Baseline Blades in a Low Speed Wind Tunnel," *17th AIAA/CEAS Aeroacoustics Conference (32nd AIAA Aeroacoustics Conference)*, Portland, OR, 05 - 08 June 2011.
6. Stephens, D.B., "Near-field Unsteady Pressure at Cruise Mach Numbers for a Model Scale Counter-Rotation Open Rotor," *18th AIAA/ CEAS Aeroacoustics Conference (33rd AIAA Aeroacoustics Conference)*, Colorado Springs, CO, 04 - 06 June 2012.
7. Stephens, D.B., "Data Summary Report for the Open Rotor Propulsion Rig Equipped with F31/A31 Rotor Blades," *NASA/TM—2014-216676*.
8. Magliozzi, B. and Hanson, D.B. and Amiet, R.K., "Propeller and Propfan Noise," Chapter 1, "Aeroacoustics of Flight Vehicles: Theory and Practice, Volume 1: Noise Sources," NASA-RP 1258, Vol. 1, August 1991.
9. Blandeau, V.P. and Joseph, P.F., "Broadband Noise due to Rotor-Wake/Rotor Interaction in Contra-Rotating Open Rotors," *AIAA Journal*, Vol. 48, No. 11, pp. 2674-2686, November 2010.
10. Parry, A.B., Kingan, M. and Tester, B.J., "Relative Importance of Open Rotor Tone and Broadband Noise Sources", *17th AIAA/CEAS Aeroacoustics Conference (32nd AIAA Aeroacoustics Conference)*, Portland, OR, 05 - 08 June 2011.
11. Sree, D., "A novel signal processing technique for separating tonal and broadband noise components from counter-rotating open-rotor acoustic data," International Journal of Aeroacoustics, Vol. 12, Issue 1/2, June 2013.
12. Sree, D. and Stephens, D.B., "Tone and Broadband Noise Separation from Acoustic Data of a Scale-Model Counter-Rotating Open Rotor," Paper No. AIAA-2014-2744, Proceedings of AIAA Aviation and Aeronautics Forum and Exposition, Atlanta, GA, June 16-20, 2014.

13. Stephens, D.B. and Envia, E. (Acoustics Branch, NASA-GRC, Cleveland, Ohio), Private communications, July 2014.
14. Janardan B.A. and Gliebe P.R., “Acoustic Power Level Comparisons of Model-Scale Counterrotating Unducted Fans,” AIAA paper 91-0595, 29th Aerospace Sciences Meeting, Reno, Nevada, January 7-10, 1991.
15. Hanson, D.B., “Sound Power Spectrum and Wave Drag of a Propeller in Flight,” AIAA 12th Aeroacoustic Conference, San Antonio, Texas, AIAA 89-1081, April 1989.